



Combined Sr, Nd, Pb and Li isotope geochemistry of alkaline lavas from northern James Ross Island (Antarctic Peninsula) and implications for back-arc magma formation

J. Košler^{a,b,*}, T. Magna^{a,b,c,1}, B. Mlčoch^b, P. Mixa^b, D. Nývlt^b, F.V. Holub^d

^a Centre for Geobiology and Department of Earth Science, University of Bergen, Allegaten 41, N-5007 Bergen, Norway

^b Czech Geological Survey, Klárov 3, CZ-118 21 Prague 1, Czech Republic

^c Institute of Mineralogy and Geochemistry, University of Lausanne, CH-1015 Lausanne, Switzerland

^d Department of Petrology and Structural Geology, Charles University, Albertov 6, CZ-128 43 Prague 2, Czech Republic

ARTICLE INFO

Article history:

Received 26 February 2008

Received in revised form 3 October 2008

Accepted 3 October 2008

Editor: R.L. Rudnick

Keywords:

Sr–Nd–Pb–Li isotopes

Back-arc magmatism

Depleted and enriched mantle

James Ross Island

Antarctic Peninsula

ABSTRACT

We present a comprehensive geochemical data set for a suite of back-arc alkaline volcanic rocks from James Ross Island Volcanic Group (JRIVG), Antarctic Peninsula. The elemental and isotopic (Sr, Nd, Pb and Li) composition of these Cenozoic basalts emplaced east of the Antarctic Peninsula is different from the compositions of the fore-arc alkaline volcanic rocks in Southern Shetlands and nearby Bransfield Strait. The variability in elemental and isotopic composition is not consistent with the JRIVG derivation from a single mantle source but rather it suggests that the magma was mainly derived from a depleted mantle with subordinate OIB-like enriched mantle component (EM II). The isotopic data are consistent with mantle melting during extension and possible roll-back of the subducted lithosphere of the Antarctic plate. Magma contamination by Triassic–Early Tertiary clastic sediments deposited in the back-arc basin was only localized and affected Li isotopic composition in two of the samples, while most of the basalts show very little variation in $\delta^7\text{Li}$ values, as anticipated for “mantle-driven” Li isotopic composition. These variations are difficult to resolve with radiogenic isotope systematics but Li isotopes may prove sensitive in tracking complex geochemical processes acting through the oceanic crust pile, including hydrothermal leaching and seawater equilibration.

© 2008 Elsevier B.V. All rights reserved.

1. Introduction

Partial melting of mantle rocks, fractional crystallization of the melts and magma contamination with crustal rocks, and especially with sediments in the back-arc basin, are the main factors that control the chemical and isotopic composition of magmas that form in the back-arc spreading centres (e.g., Woodhead et al., 1993). Many back-arc basalts also have geochemical signatures that suggest involvement of subduction processes in their petrogenesis (e.g., Woodhead et al., 1993; Gribble et al., 1998; Turner and Hawkesworth, 1998; Peate et al., 2001). Such signatures are typically linked to prior depletion of mantle source and enrichment of magmas with elements that are thought to be transported from subducted lithosphere to the mantle wedge (e.g.,

water and large ion lithophile elements). In addition, thermal and mechanical properties of lithosphere that underlies the magmatic arc and the slope of subducted slabs are also expected to control the composition of back-arc magmas (Jarrard, 1986).

Intrusions of Cenozoic volcanic rocks that occur east of the Antarctic Peninsula in Western Antarctica are often referred to as James Ross Island Volcanic Group (JRIVG, Nelson, 1966). They intrude Triassic and younger sediments deposited in the back-arc basin of the Antarctic Peninsula in the western part of the Weddell Sea in the Larsen basin (Fig. 1). The post-Gondwanan tectonic evolution of this region includes a south-east subduction of the Phoenix plate (now part of the Antarctic plate) under the continental margin of Antarctic Peninsula, collision of the Phoenix plate spreading centre with the continental margin and subsequent slowing of the plate convergence in the Tertiary and progressive diachronous migration of the subduction towards the north-east (McCarron and Larter, 1998). During the accretion and build-up of a thick accretionary wedge on the lithospheric crust, the subduction migrated north-west, away from the Antarctic Peninsula and it probably continues till today at a very slow rate (Larter, 1991). The compression due to the lithospheric convergence was later replaced by extension across the fore-arc and magmatic arc regions and it was associated with

* Corresponding author. Centre for Geobiology and Department of Earth Science, University of Bergen, Allegaten 41, N-5007 Bergen, Norway. Tel.: +47 555 83409; fax: +47 555 83660.

E-mail address: jan.kosler@geo.uib.no (J. Košler).

¹ Present address: Institut für Mineralogie, Westfälische Wilhelms-Universität Münster, Corrensstr. 24, D-48149 Münster, Germany.

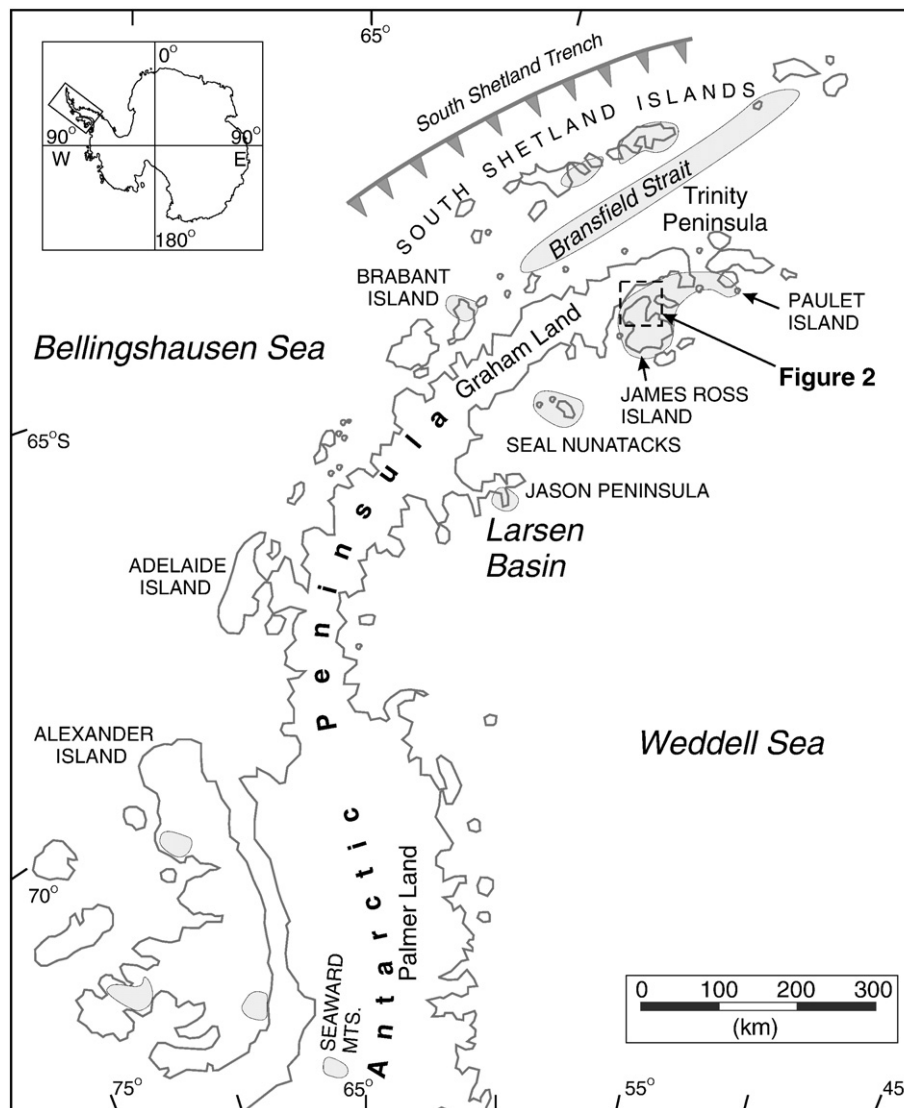


Fig. 1. Outline map of Antarctic Peninsula and adjacent islands showing major occurrences of alkaline volcanic rocks.

rifting and alkaline to calc-alkaline volcanism (McCarron and Smellie, 1998; Keller et al., 2002).

In contrast to the noticeable petrological and volcanological research in the JRIVG (Bibby, 1966; Nelson, 1966; Smellie, 1981; Sykes, 1988a; Smellie, 1999) and several dating campaigns that helped to establish the age of volcanism in the region (Sykes, 1988b; Jonkers and Kelley, 1998; Kristjánsson et al., 2005; Smellie et al., 2006a,b; Williams et al., 2006), surprisingly little is known about the chemical (Smellie, 1987; Smellie et al., 2006a) and isotopic composition of the JRIVG lavas. The available geochemical data suggest that magmas erupted in the region follow two alkaline differentiation trends: a sodium-rich and potassium-rich trend (Smellie, 1987; Smellie et al., 2006a). Lack of geochemical and, in particular, isotopic data has so far precluded a direct comparison of the JRIVG lavas with magmatic products from the other parts of the Antarctic Peninsula subduction system (cf. Hole et al., 1993; Keller et al., 2002; Fretzdorff et al., 2004).

In this paper we present new major and trace element as well as Sr–Nd–Pb–Li isotopic data for the back-arc basalts from the Antarctic Peninsula subduction system (James Ross Island Volcanic Group) to discuss the petrogenesis and magma sources and to document the differences in magma composition between arc and back-arc settings.

2. Geological setting and samples

James Ross Island (Fig. 2) is the largest single outcrop of the JRIVG, but in present-day most of the exposure of the volcanic rocks, including the island's major volcano Mt. Haddington (1638 m), is covered by an ice cap. The Ulu Peninsula in the northern part of the island represents the largest deglaciated area, with exposures of Cretaceous marine sediments (Crame et al., 1991) that were overlain by lava-fed deltas built of hyaloclastic breccias, pillow-lavas and subaerial lava flows at the top, less common tuff cones with subordinate pillow lavas, and locally penetrated by basaltic dykes and subvolcanic plugs. The age of basaltic lava-fed deltas in the Ulu Peninsula (Brandy Bay area) has been recently dated by the ^{40}Ar – ^{39}Ar technique at 6.16–3.95 Ma (Kristjánsson et al., 2005; Smellie et al., 2006b). This range, however, does not include the volcanic rocks on Cape Lachman (JR1) and the tuff cone of Bibby Point (dyke JR16).

The emplacement of alkaline volcanic rocks of the JRIVG near the northern tip of the Antarctic Peninsula along a system of block faults probably started as early as 10 Ma ago (Dingle and Lavelle, 1998; Smellie, 1999) and continued until relatively recently with the youngest recorded intrusions at ca. 130 ka (Smellie et al., 2006a).

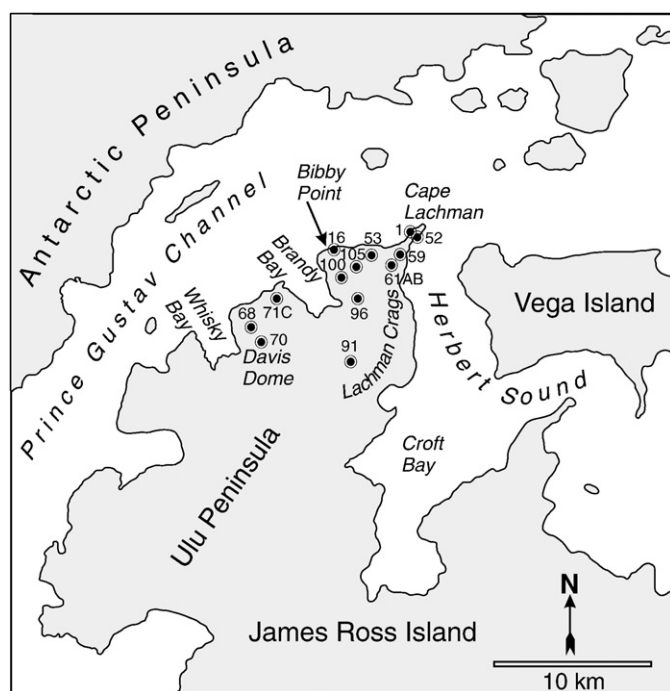


Fig. 2. Outline map of James Ross Island with locations of samples from this study.

The JRVG consists of voluminous intrusions of lavas and other volcanic products that correspond in composition to tholeiites, alkali basalts, hawaiites and rarely also to basanites and mugearites (Smellie, 1999). Volcanism in JRVG was both subaerial and submarine, with development of features typical of lava–sea water interaction, such as are pillow lavas and voluminous hyaloclastic breccias. In addition, marine fossils in some of the volcanoclastic products also suggest that some of the eruptions occurred in the marine environment while other show features indicative of magma intrusion under the inland ice cap (Smellie 2006).

Samples for this study were collected from lava flows, dykes and magma feeding channels in different parts of the Ulu Peninsula in the Brandy Bay area (Fig. 2; Cape Lachman, Lachman Crags, Bibby Point and Davis Dome). The samples comprise 14 alkaline olivine basalts and olivine dolerites (Table 1). They all have similar mineral composition but differ significantly in the mineral grain size. The olivine basalts contain phenocrysts of automorphic olivine with inclusions of Cr-rich spinel. Olivine is also present in the matrix, often together with plagioclase, clinopyroxene, magnetite and ilmenite and variable proportion of glass. Olivine dolerites are free of glass and typically contain much larger laths of plagioclase partially enclosed in clinopyroxene within the ophitic texture. Secondary constituents that are present in some JRVG basalts include various alteration products of olivine (serpentine, bowlingite), zeolite minerals in amygdules and vugs, and palagonitic alteration of glass in hyaloclastic breccias and tuffs. The samples were thoroughly checked for presence of alteration products using optical microscopy and results of major element analysis (see below). Only non-altered samples without detectable amounts of alteration products were used for petrogenetic interpretations in this study.

3. Analytical techniques

Major element composition of the basalts was determined by wet chemistry techniques in the Czech Geological Survey in Prague; basaltic standard reference materials NIST-688 and BM (ZGI Berlin) were analyzed for quality control of the measurements. The contents of Ni were measured using an ARL 9400 Advant XP X-ray fluorescence

spectrometer in the Czech Geological Survey, using the BM and JB-2 basaltic SRMs for quality control. Other trace elements and isotope analyses were carried out in the Department of Earth Science at the University of Bergen. Concentrations of trace elements and REEs were determined by solution measurements on a Thermo Finnigan Element2 ICP-MS instrument following dissolution of sample powders in a PicoTrace pressure digestion system using a mixture of HF–HNO₃ purified previously by sub-boiling distillation. Basaltic reference material BCR-2 was periodically analyzed for quality control. Results for standard reference materials analyzed for major and trace elements during the course of this study are given in the Appendix.

Powdered samples for isotope analysis were dissolved in a mixture of purified concentrated HF and HNO₃, and ion-exchange chromatography was employed to isolate Sr, Nd, Pb and Li from the sample matrix. Strontium, Pb and REE were separated by specific extraction chromatography using the technique described by Pin et al. (1994), and Nd was subsequently separated using a modified version of the method described by Richard et al. (1976). Strontium and Nd isotopes were measured on a Finnigan MAT 262 thermal ionization mass spectrometer in static mode by double Re-filament technique. Strontium isotopic ratios were corrected for mass-dependent fractionation using $^{86}\text{Sr}/^{88}\text{Sr}=0.1194$ and exponential law; Nd isotopic ratios were corrected in the same way using $^{146}\text{Nd}/^{144}\text{Nd}=0.7219$. Repeat measurements of the NBS-987 and La Jolla standards in the course of this study gave average $^{87}\text{Sr}/^{86}\text{Sr}$ and $^{143}\text{Nd}/^{144}\text{Nd}$ values of 0.710267 ± 24 and 0.511841 ± 10 (2 s.d.), respectively. Long term precision for measurements of Sr and Nd isotopic composition in NBS-987 and La Jolla standards was 0.04 and 0.02%, respectively. The total procedural blanks for Sr and Nd were lower than 50 and 10 pg, respectively and were negligible for the present study. Isotopic composition of Pb was determined by solution multi-collector ICP-MS (Thermo Finnigan Neptune) technique in static mode. Correction of Pb isotopic ratios for mass discrimination utilized exponential law and natural isotopic composition of Tl ($^{205}\text{Tl}/^{203}\text{Tl}=2.3871$) that was added to the samples prior to the analysis. Repeat measurements of the NBS-981 standard in the course of this study gave mean $^{206}\text{Pb}/^{204}\text{Pb}$, $^{207}\text{Pb}/^{204}\text{Pb}$ and $^{208}\text{Pb}/^{204}\text{Pb}$ ratios of 16.934 ± 12 , 15.484 ± 12 and 36.677 ± 29 (2 s.d.), respectively. Total procedural blank for Pb was lower than 130 pg and was always negligible.

Sample preparation and ion exchange separation of Li followed the procedure described in Magna et al. (2004). Lithium isotopic composition was determined by solution multi-collector ICP-MS in static mode and the measured isotopic ratios were corrected for instrumental mass discrimination by applying standard-sample bracketing technique. Lithium isotopic compositions of samples are expressed as $\delta^7\text{Li}$ (‰) with reference to the L-SVEC Li-carbonate standard ($^7\text{Li}/^6\text{Li}=12.02 \pm 0.03$; Flesch et al., 1973) that was used to bracket the samples during the analysis. Replicate (including full chemical separation of Li from the matrix) measurements of basaltic reference rocks JB-2, BHVO-2 and BCR-2 analyzed during the course of this study yielded $\delta^7\text{Li}=4.78 \pm 0.53\%$ (2 s.d., $n=3$), $4.58 \pm 0.58\%$ (2 s.d., $n=3$) and $3.19 \pm 0.12\%$ (2 s.d., $n=4$), respectively. This is in agreement with the published data of Tomascak et al. (1999a), Jeffcoate et al. (2004), Magna et al. (2004), Rosner et al. (2007) and others (see GeoReM at www.georem.mpch-mainz-gwdg.de, Jochum et al., 2005 for an updated list of values). Long term precision of Li isotopic measurements of JB-2 and BHVO-2 reference samples was $\sim 0.3\%$ (2 s.d.). Total procedural blank was less than 20 pg Li which and it was negligible for the analyzed samples.

4. Results

The major and trace element compositions of the JRVG samples are given in Table 1 and the corresponding major element characteristics are shown in Figs. 3 and 4. The rocks have Na₂O and K₂O contents of less than 4.0 and 1.5 wt.%, respectively, with only one olivine basalt

Table 1
Sample details and major and trace element contents in basalts from the northern part of James Ross Island

	JR1	JR16	JR52	JR53	JR59	JR61A	JR61B	JR68	JR70	JR71C	JR91	JR96	JR100	JR105
	Basalt pillow lava	Basalt dyke	Basalt pillow lava	Basalt pillow breccia	Basalt lava flow ¹⁾	Basalt lava flow	Basalt lava flow	Basalt lava flow ¹⁾	Dolerite lava flow	Dolerite volcanic plug	Dolerite dyke	Dolerite lava flow	Dolerite lava flow	Dolerite volcanic plug
South	63°47.53'	63°48.19'	63°47.82'	63°48.66'	63°48.53'	63°48.74'	63°48.74'	63°52.14'	63°52.47'	63°51.12'	63°53.17'	63°49.63'	63°49.06'	63°48.54'
West	57°48.60'	57°57.10'	57°48.05'	57°53.35'	57°49.47'	57°49.90'	57°49.90'	58°06.48'	58°04.74'	58°03.54'	57°54.18'	57°56.19'	57°56.50'	57°55.00'
<i>Major element concentrations (wt.%)</i>														
SiO ₂	46.76	45.90	46.80	48.38	48.38	48.51	48.94	46.60	48.36	47.70	48.52	48.26	47.58	48.28
TiO ₂	1.61	1.35	1.65	1.60	1.52	1.47	1.52	1.53	1.47	1.63	1.80	1.71	1.56	1.43
Al ₂ O ₃	14.70	15.73	15.31	15.40	15.09	15.48	15.52	15.62	15.45	15.91	16.49	16.47	16.01	15.38
Fe ₂ O ₃	2.11	2.27	2.07	2.03	2.38	2.61	1.90	2.79	2.49	2.03	1.87	2.17	2.05	1.91
FeO	8.75	7.04	8.46	8.44	9.09	8.79	9.64	7.76	8.13	7.75	7.72	8.23	8.65	8.74
MgO	9.93	7.03	9.32	8.72	8.94	8.53	8.54	8.85	9.29	8.32	6.75	7.55	8.79	9.48
MnO	0.19	0.17	0.18	0.18	0.18	0.18	0.18	0.18	0.18	0.18	0.17	0.18	0.18	0.19
CaO	9.03	6.91	8.19	8.38	7.33	7.75	7.78	8.41	8.78	8.43	8.92	9.59	8.61	8.33
Na ₂ O	2.93	4.52	3.41	3.06	3.43	3.55	3.80	2.84	3.22	4.09	3.96	3.42	3.44	3.55
K ₂ O	0.57	2.12	1.21	1.33	1.22	1.37	1.26	0.71	1.03	1.49	1.36	1.02	1.16	0.93
P ₂ O ₅	0.31	0.39	0.32	0.43	0.41	0.40	0.41	0.26	0.25	0.50	0.50	0.37	0.50	0.31
F	0.04	0.04	0.04	0.03	0.03	0.04	0.03	0.03	0.03	0.04	0.04	0.04	0.04	0.03
CO ₂	0.14	0.01	0.02	0.03	0.02	0.02	0.01	0.04	0.02	0.09	0.06	0.02	0.02	0.04
H ₂ O ⁺	1.51	5.34	2.41	1.50	1.41	0.99	0.28	2.85	1.06	1.57	1.55	0.68	0.92	1.00
H ₂ O ⁻	1.19	0.96	0.38	0.43	0.46	0.15	0.10	1.28	0.15	0.25	0.19	0.10	0.35	0.24
Total	99.77	99.77	99.77	99.94	99.89	99.84	99.91	99.75	99.91	99.98	99.90	99.80	99.86	99.84
<i>Trace element concentrations (ppm)</i>														
Li	5.9	n/a	6.0	4.6	6.9	6.3	6.9	6.7	5.4	6.6	7.3	4.6	7.0	6.1
Sc	25.5	25.3	25.1	22.7	19.3	18.8	19.7	25.8	24.0	24.7	25.8	26.1	25.0	23.8
V	175	165	176	157	142	142	146	180	168	180	199	179	153	164
Cr	592	317	504	459	418	431	429	515	582	533	271	432	493	599
Co	47.7	34.7	43.1	43.2	45.1	46.6	46.4	43.4	47.0	39.8	33.9	40.6	43.9	45.5
Ni	131	59	115	141	112	105	106	98	133	101	53	65	137	144
Cu	45.1	34.0	42.3	53.1	42.8	42.2	40.1	47.5	49.9	45.0	48.7	57.3	51.6	47.7
Rb	5.1	20.0	11.5	13.6	15.1	17.2	15.9	10.4	14.8	19.7	22.2	11.3	11.9	13.5
Sr	412	672	584	578	463	522	486	328	432	574	691	475	559	397
Y	24.4	23.6	24.9	24.4	23.2	22.7	23.4	24.9	24.3	25.2	26.3	25.8	25.9	22.7
Zr	145	164	148	203	169	167	171	141	163	230	217	172	180	146
Nb	20.4	29.1	21.3	35.2	31.3	30.5	31.3	16.4	22.3	41.3	43.7	24.5	29.4	23.6
Cs	0.22	0.57	0.38	0.14	0.24	0.19	0.15	0.35	0.39	0.46	0.56	0.20	0.30	0.48
Ba	96	162	106	145	141	138	139	88	129	183	214	108	151	122
Hf	3.13	3.39	3.24	4.72	3.59	3.57	3.64	3.06	3.41	4.35	4.43	3.54	3.61	3.17
Ta	1.06	1.38	1.11	1.97	1.54	1.52	1.58	0.83	1.12	1.98	2.05	1.21	1.37	1.17
Pb	2.47	3.86	2.61	4.04	2.66	2.36	2.82	2.67	2.22	2.76	3.49	1.78	2.34	n/a
Th	1.81	3.05	1.89	2.89	3.19	3.02	3.06	1.69	2.29	3.03	3.46	1.95	2.20	2.14
U	0.62	0.93	0.63	1.01	1.03	0.80	0.71	0.53	0.77	1.06	1.14	0.63	0.75	0.71
La	19.3	28.2	20.1	25.0	23.5	22.3	22.8	15.0	19.3	29.3	32.6	20.2	23.7	15.5
Ce	41.5	56.4	42.3	50.5	47.0	45.2	46.6	32.7	41.0	57.7	65.2	44.4	49.5	33.5
Pr	5.09	6.50	5.39	6.10	5.60	5.57	5.62	4.36	5.19	6.73	7.93	5.39	5.92	4.18
Nd	21.0	24.9	20.9	24.1	22.7	21.4	21.9	18.6	21.0	26.3	30.8	22.0	23.2	17.3
Sm	4.85	5.44	5.02	5.54	5.07	4.91	5.06	4.74	4.91	5.86	6.64	5.25	5.37	4.34
Eu	1.71	1.78	1.69	1.87	1.70	1.66	1.69	1.68	1.65	1.94	2.17	1.87	1.77	1.46
Gd	3.77	4.28	3.88	4.85	4.20	4.26	4.33	3.91	4.10	5.18	5.94	4.48	5.13	4.43
Tb	0.64	0.70	0.63	0.80	0.68	0.70	0.70	0.64	0.66	0.80	0.95	0.71	0.76	0.66
Dy	4.73	4.68	4.81	4.80	4.45	4.30	4.44	4.74	4.75	4.96	5.43	4.97	4.66	4.08
Ho	0.98	0.96	1.00	0.94	0.86	0.84	0.88	0.97	0.95	0.99	1.05	1.01	0.92	0.81
Er	2.88	3.00	2.89	3.00	2.70	2.67	2.67	2.83	2.81	3.19	3.42	2.99	2.56	2.23
Tm	0.39	0.39	0.39	0.36	0.33	0.33	0.33	0.38	0.36	0.39	0.40	0.40	0.35	0.31
Yb	2.58	2.53	2.57	2.49	2.22	2.12	2.25	2.53	2.44	2.63	2.72	2.68	2.26	1.99
Lu	0.38	0.38	0.37	0.35	0.32	0.30	0.31	0.36	0.35	0.37	0.38	0.38	0.33	0.29

All lava flows are subaerial except for samples marked¹⁾ that correspond to lavas deposited below subaquatic hyaloclastic breccias.

(hawaiite, sample JR16) having elevated contents of alkali elements (see Table 1). This sample contains >5 wt.% H₂O⁺ and abundant zeolite group minerals, indicative of its alteration. Although we report the geochemical data for this altered basalt, we did not use its composition for interpreting the petrogenesis of the basalts. The K₂O/Na₂O ratios are higher compared to the volcanic rocks from the South Shetland Islands, two geochemical groups of lavas from Deception Island and most rocks from the Bransfield Strait. They belong to the potassium-rich trend as previously defined for the rocks of JRIVG (Fig. 4; Smellie, 1987; Smellie et al., 2006a), and their K₂O contents at low SiO₂ contents resemble the composition of alkali basalts from the Bransfield Strait (Fig. 3; Fretzdorff

et al., 2004). The JRIVG basalts show ca. 20–90-fold enrichment in incompatible elements, including light REEs and deviate significantly from the composition of N-MORB and E-MORB (Figs. 5 and 6). While trace element patterns follow the composition of OIB, marked depletion in Rb, Ba, Th, P and also HREE (see Fig. 5) makes the JRIVG lavas distinct from the composition of other OIBs. Also, lack of depletion in high-field-strength elements (e.g., Nb in Fig. 5) and higher contents of LREEs discriminate the composition of the JRIVG lavas from the composition of basaltic melts associated with magmatic arc settings (cf. Figs. 5 and 6). Unlike the enrichment in Pb and Sr, which is consistent for all JRIVG samples in this study, the extent of the K anomaly is more variable,

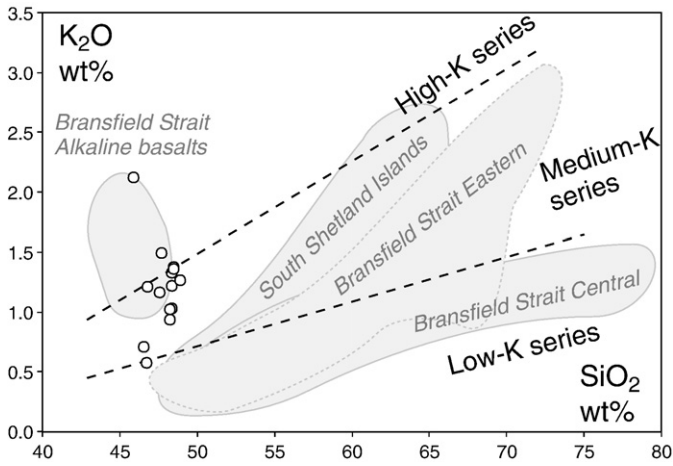


Fig. 3. Major element contents in olivine basalts from the northern part of James Ross Island showing their K-rich composition. Compositional fields for the Bransfield Strait and South Shetland Islands are plotted for comparison and are based on data of Tarney et al. (1982), Saunders and Tarney (1984), Smellie et al. (1984), Fisk (1990), Keller et al. (1992, 2002) and Fretzdorff et al. (2004). Composition field boundaries are based on Peccerillo and Taylor (1976).

ranging from a strong enrichment (altered sample JR16) to a slight depletion in one sample (JR1). The Nb/Yb–Th/Yb compositions plot along the MORB–OIB array of Pearce and Peate (1995) with some, but not all samples overlapping compositional field of alkaline basalts from the Bransfield Strait (Fretzdorff et al., 2004; Fig. 7). The JRIVG suite differs significantly from other (non alkaline) lavas from the Bransfield Strait that have, consistently with their derivation from magmatic arc setting, higher Th and lower Nb contents.

The isotopic composition of Sr, Nd and Pb is given in Table 2 and shown in Fig. 8. The isotopic data in these plots have not been age corrected. However, given the Rb/Sr and Sm/Nd ratios, and the low U contents (mostly less than 1 ppm) in the samples, an age correction up to 6.16 Ma (i.e., the maximum reported age for samples from the area,

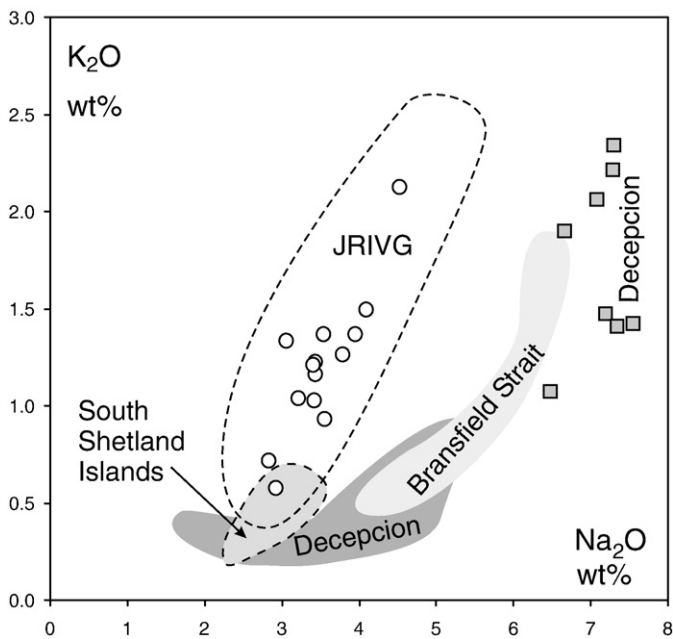


Fig. 4. Variation in alkali element contents in olivine basalts from the northern part of James Ross Island. Compositions of other alkaline Quaternary volcanic rocks are plotted for comparison based on data in Keller et al. (2002) and Smellie et al. (2006a, b). Dashed line delimits the composition of JRIVG as analyzed by Smellie et al. (2006a).

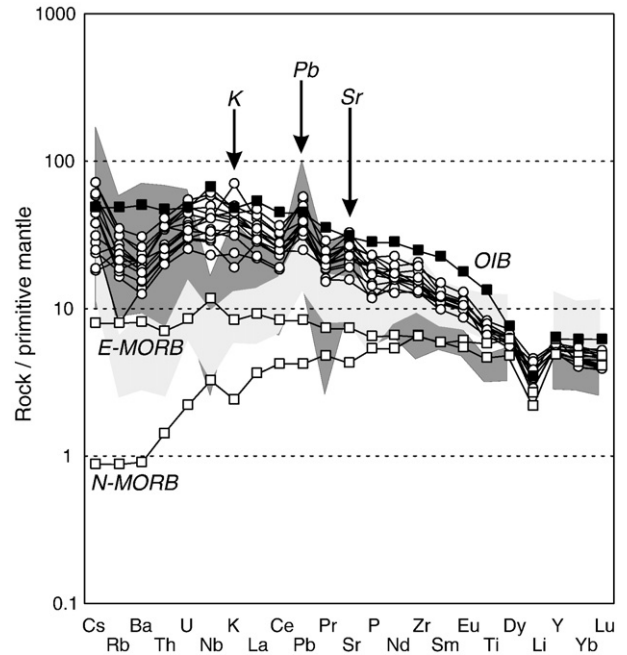


Fig. 5. Trace element composition of olivine basalts from the northern part of James Ross Island. Data are normalized to the composition of primitive mantle (Sun and McDonough, 1989). The dark grey field represents the range of compositions of various arc basalts (Kelemen et al., 2003), the light grey field corresponds to the composition of volcanic rocks from the Bransfield Strait (Keller et al., 2002). Trace element patterns of MORB and OIB are from Sun and McDonough (1989).

Kristjánsson et al., 2005) would not change the Sr, Nd and Pb isotopic ratios outside the quoted analytical uncertainties. The Sr and Nd isotopic composition of most of the basalts is uniform and the data plot in a tight

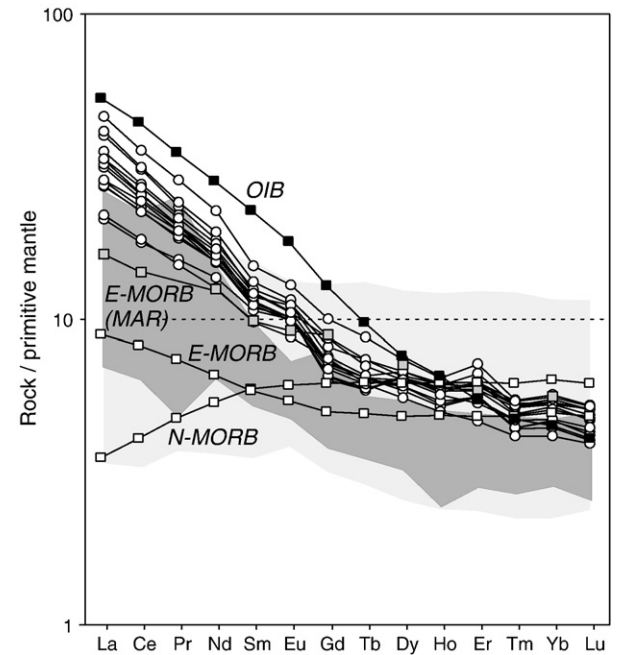


Fig. 6. Rare earth element composition of olivine basalts from the northern part of James Ross Island. Data are normalized to the composition of primitive mantle (Sun and McDonough, 1989). The dark grey field represents the range of compositions of various arc basalts (Kelemen et al., 2003), the light grey field corresponds to the composition of volcanic rocks from the Bransfield Strait (Keller et al., 2002). REE patterns of MORB and OIB are from Sun and McDonough (1989), the composition of MORB from Mid-Atlantic Ridge (MAR) is from the compilation by Klein (2003).

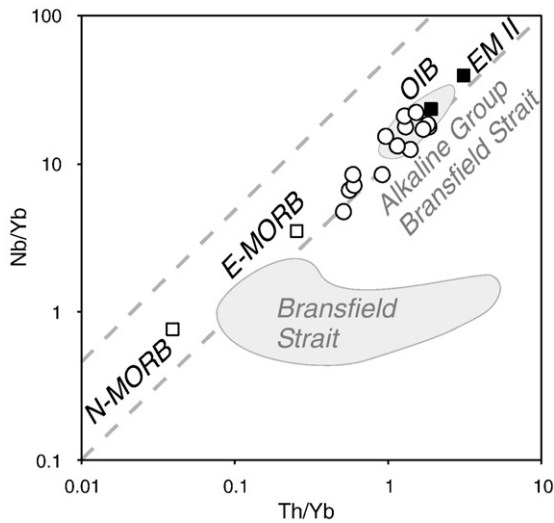


Fig. 7. Nb/Yb versus Th/Yb plot showing the composition of olivine basalts from the northern part of James Ross Island. Also shown is the composition of volcanic rocks from the Bransfield Strait (Keller et al., 2002; Fretzdorff et al., 2004). Compositions of MORB and OIB are from Sun and McDonough (1989), composition of enriched mantle EMII is from Armienti and Gasperini (2007), dashed lines delimit the MORB–OIB array of Pearce and Peate (1995).

cluster in Fig. 8a with epsilon Sr and epsilon Nd values ranging from ca. –19 to –21 and +4.4 to +5.2, respectively. Only two samples (altered basalt JR16 and JR52) have somewhat different Sr isotopic composition with epsilon values of –11 and –14, respectively. In addition, the sample JR16 also differs by 1.5 epsilon units from the mean Nd isotopic composition of all other basalts. Except for these two samples, the isotopic composition of Sr and Nd in the JRIVG suite corresponds well to the isotopic composition of alkaline volcanic rocks from the Antarctic Peninsula (Hole et al., 1993) or straddles the boundary between the composition of the Antarctic Peninsula alkaline volcanics, and alkaline volcanic rocks from the eastern part of the Bransfield strait (Fretzdorff et al., 2004) and those from the South Shetland Islands (Fig. 8a; see Keller et al., 2002 and Fretzdorff et al., 2004 for complete list of references). The Pb isotopic composition is more radiogenic compared to the volcanic rocks from South Shetland Islands and from the Bransfield Strait (Fig. 8b). Similarly, it also corresponds to the composition of alkaline basalts from the Antarctic Peninsula with only two exceptions (samples JR100 and JR105) that have Pb isotopic composition rather similar to the volcanic rocks from the Bransfield Strait. Isotopic composition of Li in the JRIVG samples varies between +1.6‰ and +6.9‰. The Li isotopic data for 12 out of 14 samples fall in a limited range with average $\delta^7\text{Li} = +3.9 \pm 0.9\%$ (2 s.d.) which is indistinguishable from the Li isotopic composition of rocks

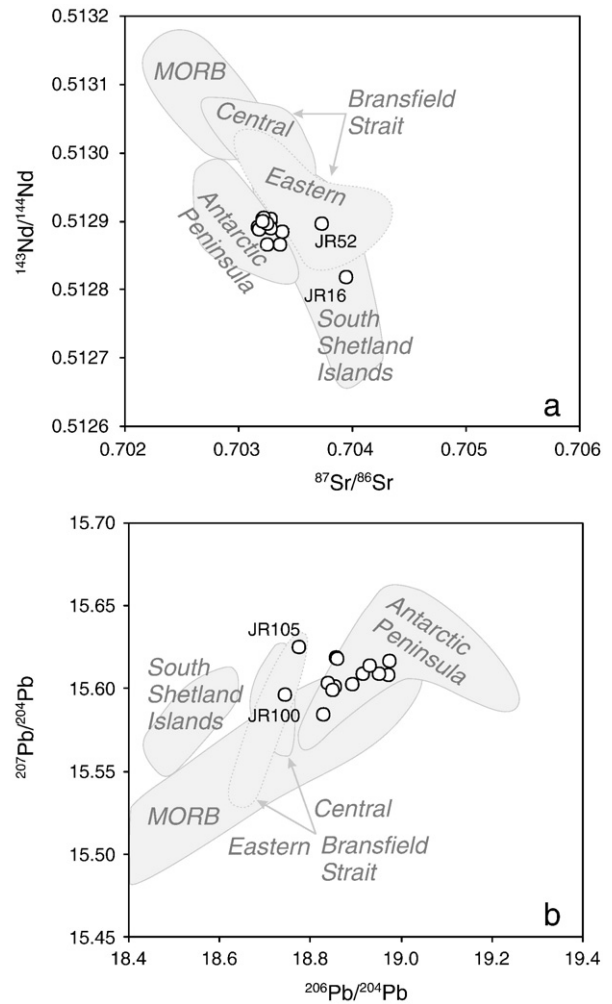


Fig. 8. Isotopic composition of (a.) Sr and Nd and (b.) Pb of olivine basalts from the northern part of James Ross Island. Analytical uncertainties are within the size of the plotted symbols. Also shown are fields for lavas from the central and eastern Bransfield Basin, South Shetland Islands, Antarctic Peninsula alkali basalts and MORB. Sources of data are as in Fig. 3 with additional data from Hanan et al. (1986), Hole (1990), Birkenmajer et al. (1991), and Guangfu et al. (1997).

associated with magmatic arcs (Tomascak et al., 2002; Leeman et al., 2004), mid-ocean ridge settings (Elliott et al., 2006; Tomascak et al., 2008) and terrestrial mantle (Magna et al., 2006b; Jeffcoate et al., 2007). No significant co-variation exists between $\delta^7\text{Li}$ and compositional

Table 2
Strontium, Nd, Pb and Li isotopic composition of basalts from the northern part of James Ross Island

Sample	$^{87}\text{Sr}/^{86}\text{Sr}$	± 2 sigma	$\epsilon\text{Sr}_{\text{UR}}$	$^{143}\text{Nd}/^{144}\text{Nd}$	± 2 sigma	$\epsilon\text{Nd}_{\text{CHUR}}$	$^{206}\text{Pb}/^{204}\text{Pb}$	± 2 sigma	$^{207}\text{Pb}/^{204}\text{Pb}$	± 2 sigma	$^{208}\text{Pb}/^{204}\text{Pb}$	± 2 sigma	$\delta^7\text{Li}$ (‰)	± 2 sigma
JR1	0.703387	0.000009	-18.6	0.512884	0.000005	4.8	18.855	0.001	15.601	0.001	38.556	0.003	3.6	0.3
JR16	0.703948	0.000008	-10.7	0.512818	0.000005	3.5	18.857	0.001	15.619	0.001	38.644	0.002	n/a	n/a
JR52	0.703737	0.000009	-13.7	0.512896	0.000005	5.0	18.841	0.001	15.603	0.001	38.544	0.003	3.3	0.1
JR53	0.703281	0.000008	-20.1	0.512903	0.000005	5.2	18.859	0.001	15.618	0.001	38.617	0.002	1.5	0.2
JR59	0.703216	0.000008	-21.1	0.512891	0.000005	4.9	18.916	0.001	15.608	0.001	38.626	0.003	4.0	0.1
JR61A	0.703281	0.000008	-20.1	0.512889	0.000004	4.9	18.972	0.001	15.608	0.001	38.658	0.003	3.9	0.1
JR61B	0.703175	0.000009	-21.6	0.512890	0.000006	4.9	18.953	0.001	15.608	0.001	38.637	0.002	3.4	0.1
JR68	0.703188	0.000009	-21.5	0.512888	0.000005	4.9	18.932	0.001	15.614	0.001	38.646	0.003	4.0	0.1
JR70	0.703256	0.000008	-20.5	0.512866	0.000005	4.4	18.974	0.001	15.616	0.001	38.692	0.002	4.0	0.1
JR71C	0.703211	0.000008	-21.1	0.512903	0.000005	5.2	18.829	0.001	15.584	0.001	38.463	0.002	4.3	0.2
JR91	0.703222	0.000007	-21.0	0.512905	0.000005	5.2	18.849	0.001	15.599	0.001	38.549	0.002	4.2	0.1
JR96	0.703256	0.000008	-20.5	0.512895	0.000005	5.0	18.894	0.001	15.602	0.001	38.554	0.003	6.8	0.1
JR100	0.703216	0.000008	-21.1	0.512899	0.000005	5.1	18.745	0.001	15.596	0.001	38.470	0.003	4.9	0.1
JR105	0.703369	0.000008	-18.9	0.512866	0.000006	4.4	18.775	0.001	15.625	0.001	38.531	0.002	3.6	0.1

Analytical uncertainties are given as 2 sigma (internal). Lithium isotopic composition is expressed relative to the L-SVEC Li isotopic standard, data in brackets correspond to replicate (including ion exchange separation) measurements of Li isotopic composition.

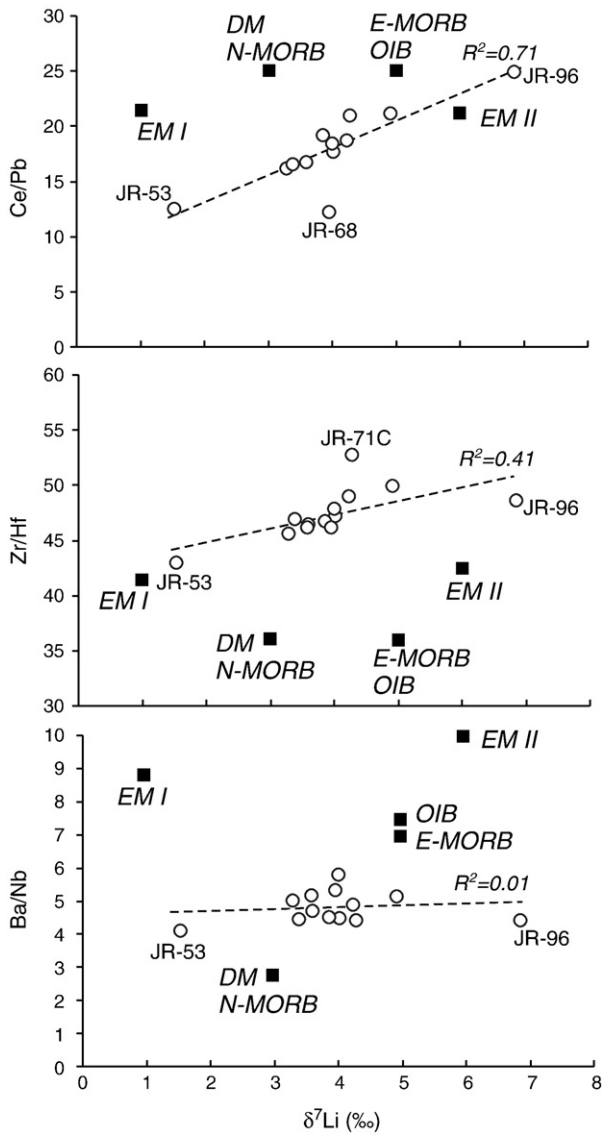


Fig. 9. Lithium isotopes vs. trace element compositions of olivine basalts from the northern part of James Ross Island. Elemental ratios of LREE/Pb all mimic the pattern of Ce/Pb vs. $\delta^7\text{Li}$ shown in the figure. Also shown are reported mean composition values of MORB, OIB and mantle end members from Sun and McDonough (1989), Armienti and Gasperini (2007) and Nishio et al. (2007).

parameters that are typical of subduction settings (e.g., Ba/Nb, Ba/La and Sr/Y); $\delta^7\text{Li}$ shows a weak correlation with indices of crustal assimilation and/or crystal fractionation, e.g., LREE/Pb (Fig. 9). This is, however, largely controlled by two samples with extreme $\delta^7\text{Li}$.

Collectively, the JRIVG alkaline basaltic lavas are geochemically different from the subduction (arc)-related magmatic rocks from the Bransfield Strait and from the Antarctic Peninsula. The main differences found in the lavas from James Ross Island include higher K/Na ratio, higher content of incompatible elements, lack of a negative Nb anomaly and more radiogenic isotopic composition of Pb (compared to the rocks found in Southern Shetlands and Bransfield Strait).

5. Discussion

5.1. Origin of alkaline magmas in the Antarctic Peninsula subduction system

Products of alkaline magmatism along the Antarctic Peninsula subduction system were found on South Shetland Islands, in Bransfield

Strait, on Brabant Island, on James Ross Island and the adjacent archipelago as far to the north-east as Paulet Island, on Seal Nunataks, on Jason Peninsula, and further south in the Palmer Land on Alexander Island, Seaward Mountains, Merrick Mountains and Rydberg Peninsula (Fig. 1; Smellie, 1987; Hole, 1988, 1990; Hole et al., 1991a,b; Smellie, 1999; Fretzdorff et al., 2004). The age of alkaline magmatism varies from recent to ca. 54 Ma on Alexander Island. There, the formation of alkaline magma has been attributed to opening of a slab window beneath the Antarctic Peninsula, upwelling of a non-altered asthenospheric mantle and decompression melting that started in the garnet stability field and led to the formation of alkaline basaltic magma (Hole et al., 1991b, 1995). Variety of alkaline magmas could have formed from two asthenospheric mantle sources: (i) by partial melting of shallow convecting MORB-like asthenosphere beneath the Antarctic Peninsula and (ii) from a deep-seated mantle plume beneath the West Antarctic rift system, which produced basaltic magma as a result of plume rise and decompression melting. This model assumes very little or no contribution from the subducting slab to the mantle-derived magma (Hole and LeMasurier, 1994 and references therein). While this process can explain formation of alkaline magma on Alexander Island, it is unlikely for the origin of other occurrences of alkaline rocks further north where it is not consistent with the available geophysical evidence and where the lava eruptions are significantly younger (see discussion in Fretzdorff et al., 2004). Alternative models were proposed to explain the formation and variability in geochemical composition of alkaline and sub-alkaline magmas associated with the Antarctic Peninsula subduction system.

(i) The alkaline magmatism in the JRIVG originated by low but variable degrees (<3%) of partial melting of garnet-bearing mantle and the composition of the melt was further modified by fractional crystallization of olivine and clinopyroxene. Although there is no clear temporal association of the alkaline magmatism with the within-plate setting (e.g., migration of the plate over a stationary mantle hot-spot), regional extension was a prerequisite for magma ascent to the surface (Smellie, 1987).

(ii) The sub-alkaline magma formation in the Bransfield Strait has been explained by melting of a MORB-like mantle source contaminated by variable amounts (up to 5%) of subduction-related component, either metalliferous sediments (Keller et al., 2002) or LILE-rich fluid with radiogenic Sr, Nd and Pb isotope compositions derived predominantly from subducted sediments (Fretzdorff et al., 2004). Lee et al. (2008) explain the formation of volcanic rocks of the South Shetland Islands by addition of a relatively constant subduction component to temporally varying heterogeneous mantle sources. On the other hand, the formation of alkaline magma in the Bransfield Strait is assumed to involve upwelling and decompression melting of fresh asthenospheric mantle without much contribution from a subduction-modified lithosphere (Fretzdorff et al., 2004). This has been attributed to a roll-back at the South Shetland Trench (cf. Barker and Austin, 1998), possibly associated with extension and propagation of the South Scotia Ridge fault westward and with transtension across the Bransfield basin. This extension could have been coupled to a roll-back of the oceanic lithosphere that was subducted from the NE, resulting in upwelling and melting of asthenosphere and mixing of the melts with MORB-like crust underneath what has later become the JRIVG (Hole et al., 1995).

5.2. Origin of alkaline rocks from the northern part of James Ross Island

Compared to the geochemical signatures of alkaline rocks discussed in the previous section, a model of magma formation for olivine basalts from the northern part of James Ross Island must also account for elevated contents of incompatible elements, as well as for a significantly more radiogenic isotopic composition of Pb and the observed range of Li isotopic compositions. The level of trace element enrichment is significantly higher compared to that of volcanic rocks

from the Bransfield Strait (Keller et al., 2002; Fretzdorff et al., 2004) and markedly different from the composition of the N-MORB both from MAR and EPR (cf. Klein, 2003). A simple two-component mixing model similar to that used by Keller et al. (2002) has been attempted to explain the composition of the JRIVG samples (Fig. 10). Similar to Keller et al. (2002), we have assumed a depleted mantle (DM) composition end-member ($^{87}\text{Sr}/^{86}\text{Sr}=0.7025$, $\text{Sr}=20$ ppm, $^{143}\text{Nd}/^{144}\text{Nd}=0.5132$, $\text{Nd}=1.1$ ppm, $^{206}\text{Pb}/^{204}\text{Pb}=17.60$, $\text{Pb}=0.043$ ppm; cf. Keller et al., 2002) and two potential sedimentary contaminants: an average Atlantic sediment ($^{87}\text{Sr}/^{86}\text{Sr}=0.7092$, $\text{Sr}=150$ ppm, $^{143}\text{Nd}/^{144}\text{Nd}=0.5124$, $\text{Nd}=20$ ppm, $^{206}\text{Pb}/^{204}\text{Pb}=18.63$, $\text{Pb}=14$ ppm; Ben Othman et al., 1989) and a metalliferous sediment ($^{87}\text{Sr}/^{86}\text{Sr}=0.7090$, $\text{Sr}=200$ ppm, $^{143}\text{Nd}/^{144}\text{Nd}=0.5124$, $\text{Nd}=20$ ppm, $^{206}\text{Pb}/^{204}\text{Pb}=18.75$, $\text{Pb}=200$ ppm; cf. Keller et al., 2002). Results of modelling suggest that the composition of JRIVG lavas cannot be easily explained by a binary mixing between depleted mantle-derived magma and average Atlantic sediment (Fig. 10). A similar model based on the composition of a depleted mantle source mixed with less than 5% of a contaminant corresponding in composition to a metalliferous sediment (i.e., an average Atlantic sediment with ca. 14-fold Pb content) can explain the composition of basaltic rocks from the Bransfield Strait reported by Keller et al. (2002), as well as most of the samples from the same region reported by Fretzdorff et al. (2004). The calculated mixing

curve in Fig. 10 does not, however, explain the composition of most of the basalts from JRIVG because a significantly more radiogenic Pb composition of the contaminant would be required. This is consistent with the trace element contents that suggest very little (if any) contribution of the slab-derived material to the mantle-derived magma (cf. Fig. 7) but rather it points to a combination of a depleted mantle (e.g., E-MORB)-derived magma with an OIB-like source, such as is the enriched mantle component EMII (Zindler and Hart, 1986). This is further endorsed by trace element systematics (e.g., Ba–Th–La–Nb–Sm; cf. Kent and Elliott, 2002; Plank, 2005) where all data fall in the MORB–OIB field and far away from sediments and/or arc volcanics. Contrary to this, Lee et al. (2008) have shown that a great proportion of fluid mobile elements in sub-alkaline lavas from South Sandwich Islands (~200 km NNW) were derived from a subducted altered crust component. Therefore, when combined with our data, progressively decreasing input of fluid phase originated from subducting plate into the melting region provides evidence of drastically reduced role of sedimentary component in generation of back-arc volcanics.

In contrast to the contamination of depleted mantle component by sediments, its mixing with ca. 25–35 wt.% of enriched mantle component, such as is EMII (assuming $\text{Pb}/\text{Sr}/\text{Nd}=1/10/2$ and $^{87}\text{Sr}/^{86}\text{Sr}=0.7078$, $^{143}\text{Nd}/^{144}\text{Nd}=0.5126$, $^{206}\text{Pb}/^{204}\text{Pb}=19$; Armienti and Gasperini, 2007; Fig. 10), can explain the composition of the bulk of the JRIVG lavas. The somewhat higher proportion of enriched mantle component required to model the composition of the JRIVG lavas in the Pb–Nd system compared to the Pb–Sr mixing may reflect Sr–Nd elemental decoupling during the melting. Small variations in the isotopic compositions of Sr and Nd might reflect variable proportions of the two main magma sources in the mixture. Interestingly, most of the samples plot within the composition field of alkaline basalts from the Antarctic Peninsula in Fig. 10 (Hole, 1990; Hole et al., 1993; cf. also Keller et al., 2002), i.e., they contain substantially more radiogenic Pb than samples from other back-arc settings, such as are the Japan Sea, the Mariana Trough or the Scotia Arc (cf. Fig. 10).

Although some of the observed Sr, Nd and Pb isotopic signatures could be explained by contamination of MORB-like magma with a more geochemically evolved material of the Antarctic Peninsula crust, this is not consistent with their trace element signatures, Li isotopic composition and field or geophysical information. There is no direct evidence (e.g., seismic data or occurrence of xenoliths in volcanic rocks) of the crustal rocks from the northern part of the Antarctic Peninsula extending further east beyond the Prince Gustav Channel and forming a basement of the Triassic–Tertiary sediments in the James Ross Basin, although similarities exist between the northern part of Antarctic Peninsula (Graham Land) and southern South America (e.g., Magallanes Basin) where the volcanic and plutonic basement rocks extend east of the cordillera and partly underlie the back-arc basin (see discussion in Hathway, 2000). Alternatively, a magma contamination by the Triassic–Tertiary clastic sedimentary rocks that occur in the James Ross Basin and that were derived from the Antarctic Peninsula (Pirrie, 1994) could have also provided the radiogenic Pb for the mantle-derived parent magma of the JRIVG basalts. Field evidence for variable contamination of basaltic magma by sediments was found on several outcrops during this study. It varies from occurrence of sedimentary xenoliths in the basalts to partial and sometimes almost complete melting of the sedimentary xenoliths and sediments adjacent to magma intrusions. The available data do not allow for a quantitative estimate of the sediment contribution to the magma but our field observations suggest that assimilation of the sediments did not have a profound effect on the composition of the JRIVG lavas.

5.3. Lithium isotopes in JRIVG lavas

Lithium isotopes have been used to unravel processes of seafloor alteration, subduction, dehydration and arc volcanism (Chan et al.,

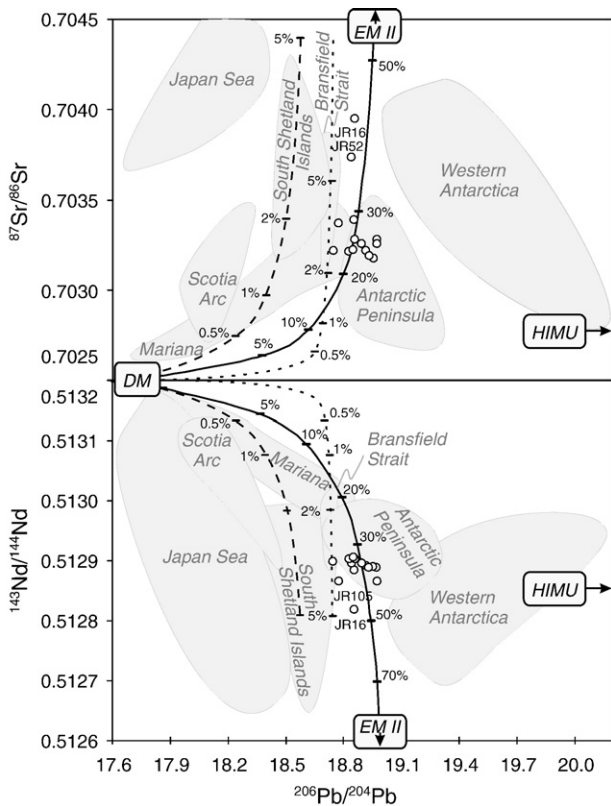


Fig. 10. Strontium, Nd and Pb isotopic composition of olivine basalts from the northern part of James Ross Island. Dashed, dotted and solid lines represent mixing between depleted mantle composition (DM) and average Atlantic sediment, metalliferous sediment and enriched mantle component (EMII; Armienti and Gasperini, 2007), respectively. The numbers next to mixing curves correspond to the weight percent contribution from the sediments (see text and Keller et al., 2002 for more details) and enriched mantle, respectively. Analytical uncertainties are within the size of the plotted symbols. Also shown are compositional fields for volcanic rocks from Japan Sea (Cousens and Allan, 1992), Mariana Trough (Hawkins et al., 1990; Stern et al., 1990; Volpe et al., 1990), East Scotia arc (Saunders and Tarney, 1979; Cohen and O'Nions, 1982; Leat et al., 2000), Antarctic Peninsula (Hole, 1990; Hole et al., 1993), various intrusions in western Antarctica (Hart et al., 1995; Rocholl et al., 1995) and Bransfield Strait (Keller et al., 2002). HIMU and EMII are radiogenic Pb mantle components of Zindler and Hart (1986).

1992, 2002; Tomascak et al., 2002; Zack et al., 2003; Magna et al., 2006a; Marschall et al., 2007) but there are only limited data for lavas from the back-arc. Lithium isotopic compositions of back-arc lavas both from High-Cascades (Leeman et al., 2004) and north-eastern Japan (Moriguti et al., 2004) are indistinguishable from the composition of lavas in this study. In particular, chemical similarities are observed for the JRIVG samples and Group I as defined in Leeman et al. (2004), especially in Ba/Nb, Li/Y, radiogenic isotopes and $\delta^7\text{Li}$. Leeman et al. (2004) explained the observed composition as a result of decompression melting of convectively upwelling asthenospheric mantle that underwent only minor modifications from its primary MORB–OIB source composition. These observations are consistent with the observed restricted range of Li isotopic compositions in JRIVG lavas (except for two samples with lighter and heavier $\delta^7\text{Li}$, respectively; see discussion below) and largely dominant role of a depleted mantle source having $\delta^7\text{Li}$ close to the reported mantle range of +3 to +4‰ (Magna et al., 2006b; Jeffcoate et al., 2007; Seitz et al., 2007; Tomascak et al., 2008). Melting of such mantle domain would most likely cause no or very limited Li isotope fractionation not beyond analytical uncertainties (Tomascak et al., 1999b). These basaltic melts would be dominated by Li from asthenospheric mantle with $\delta^7\text{Li}$ effectively identical to their precursor(s), and only large contribution of Li-enriched material with distinct Li isotopic composition might modify the intrinsic $\delta^7\text{Li}$ of the original mantle source. The hypothesis inferred from clinopyroxene data of Nishio et al. (2004) that suggests dramatic departure of Li isotopic composition in enriched mantle domains (down to -17%) from the average MORB or upper mantle composition has been recently flawed (Jeffcoate et al., 2007; Rudnick and Ionov 2007). In addition, the absence of isotopically exotic composition in OIB is supported by limited data that yield similar range of $\delta^7\text{Li}$ values to that reported for global MORBs (Tomascak et al., 1999b; Chan and Frey, 2003; Tomascak et al., 2008). Lithium isotopic composition from a suite of intra-plate volcanic rocks from the Crary Mountains on Ross Island has been reported by Ryan and Kyle (2004). These rocks have similar major and trace element compositions to JRIVG and they have highly radiogenic Pb isotopes close to HIMU that was interpreted as originating from an enriched mantle domain. However, a comparison of magma formation in the Crary Mountains and JRIVG is problematic because of different geological settings and large distance between these terrains.

The isotopic compositions of Li in two samples with apparently distinct $\delta^7\text{Li}$ (JR-53 and JR-96) require different explanations. The combined isotopic Sr–Nd–Pb modelling invokes an addition of 25–35 wt.% of EMII-like component to the JRIVG magma (Fig. 10). The Li isotope inventory of EMII is not well constrained but the isotopic variations are unlikely to exceed few per mil units. Limited data for EMII-like lavas from the French Polynesia (Chan et al., Earth Planet. Sci. Lett., under review) yield $\delta^7\text{Li}$ values between +3.8 and 5.9‰. Accordingly, the required contribution of such component would not affect the isotopic composition of Li significantly. Modeling of the radiogenic isotope composition in the JRIVG suite (Fig. 10) also suggests that relatively large amount of sedimentary contaminant (~5 wt.%) would be required to significantly modify the Sr–Nd–Pb isotopic composition of the mantle-derived magma. In contrast, due to large Li concentrations in most sediments (up to ca. 80 ppm in clay-rich silts; Chan et al., 2006) and their variable $\delta^7\text{Li}$ ranging from -4 to $+15\%$ (Moriguti and Nakamura, 1998; Bouman et al., 2004; Teng et al., 2004; Chan et al., 2006), even small and often localized contamination of magma by sedimentary material may affect the Li content and isotopic composition of the lavas. Variable proportion of sediments can be inferred from weak positive correlations of $\delta^7\text{Li}$ with LREE/Pb (Fig. 9). It is suggested that a Pb-rich sedimentary component may contain isotopically light Li because the high Pb/LREE in JR-53 is due to significantly higher Pb contents relative to other JRIVG rocks while LREE abundances are nearly constant for the whole JRIVG suite. A low $\delta^7\text{Li}$ of $<+3\%$ has been recognised in the South Sandwich sediments,

geographically close to the Antarctic Peninsula and also in clays from the back-arc setting in the Banda region (Bouman et al., 2004; Chan et al., 2006). Isotopically lighter $\delta^7\text{Li}$ in JR-53 could have resulted from incorporation of a small amount of such sedimentary material. Conversely, the isotopically heavy Li recorded in sample JR-96 is accompanied by the lowest Pb content found in the suite of studied samples. This may be indicative of incorporation of small amount of hydrothermally altered oceanic crust that lost some of its original Li and Pb inventory and that re-equilibrated subsequently with seawater. Such modified oceanic crust is expected to be isotopically heavy, with low Li and Pb contents, consistent with Li isotope systematics of the oceanic crust profile described by Chan et al. (2002).

6. Concluding remarks

The isotopic compositions and major and trace element contents in olivine basalts from the back-arc basin exposed in the northern part of James Ross Island are fairly homogeneous, except for only few outliers. They are indicative of ca. 25–35 wt.% contribution of an enriched mantle component to a MORB-like depleted mantle with no significant contribution of sedimentary material from the subducted oceanic lithosphere of the Antarctic plate. Limited number of samples shows variations in contents of trace elements and also Li isotopes, and to a minor extent also Sr and Pb isotopes but these are interpreted as resulting from localized contamination of the magma by Triassic–Tertiary clastic sediments at a late stage of the lava emplacement. Composition of the JRIVG lavas is different from the composition of other volcanic rocks in this region, in particular basaltic rocks that form the South Shetland Islands (e.g., Machado et al., 2005 and references therein) and the ocean floor in the Bransfield Strait (Keller et al., 2002; Fretzdorff et al., 2004) that have lower $\text{K}_2\text{O}/\text{Na}_2\text{O}$ ratios, lower contents of incompatible elements and less radiogenic isotopic composition of Pb. These differences are attributed mainly to the presence of a slab-derived component in the rocks of South Shetland Islands and Bransfield Strait. The K-enrichment in the JRIVG basalts relative to other volcanic rocks in the area (Fig. 4) most likely reflects different magma sources and low-degree partial melting in the enriched mantle component that contributed to the JRIVG lavas. The presence of enriched mantle component in the back-arc lavas from James Ross Island and its lack in the magmatic rocks found west of the Antarctic Peninsula are consistent with the model of regional extension linked to the roll-back of the subducted slab of Antarctic plate (cf. cartoon on Fig. 10, Hole et al., 1995). In this model, the roll-back of the trench resulted in upwelling and melting of the enriched mantle asthenosphere and mixing of the melts with MORB-like crust underneath the JRIVG. Consistently with the available data, the contribution of a slab-derived component in this model should increase towards the trench. The newly obtained geochemical data point to the importance of tectonic control during the formation of alkaline volcanic rocks in the JRIVG in western Antarctica.

Acknowledgements

This project has been financially supported by R&D project no. VaV/660/1/03 funded by the Czech Ministry of the Environment. The ICP-MS facility at the University of Bergen is supported by the Research Council of Norway. We thank the Fuerza Aerea Argentina for logistical support during the field seasons 2004–2005. Paul Tomascak and an anonymous reviewer provided useful comments that helped to improve the quality of this paper. We are grateful to Roberta Rudnick for editorial handling.

Appendix A. Details of major and trace element analysis

Major element concentrations were determined after combined HF– HNO_3 digestion of rock powder by the following techniques:

Table A1

Measured and reference values (GeoReM; Jochum et al., 2005) for standard reference materials analyzed during this study

NIST-688 (wt.%), standard deviation calculated from 20 replicate measurements					
	Measured values		GeoReM values		
	Measured	1 s.d.	Range		
SiO ₂	47.99	0.16	48.35–48.40, 2 values		
TiO ₂	1.12	0.04	1.168–1.17, 2 values		
Al ₂ O ₃	17.18	0.06	17.35–17.36, 2 values		
Fe ₂ O ₃	10.03	0.09	10.08–10.28, 2 values		
FeO	7.42	0.07	7.57		
MnO	0.167	0.004	0.167		
Na ₂ O	2.02	0.03	2.05–2.16, 2 values		
K ₂ O	0.196	0.013	0.187–0.19, 2 values		
P ₂ O ₅	0.133	0.006	0.133–0.134, 2 values		
ZGI-BM (wt.%), standard deviation calculated from 14 replicate measurements					
	Measured values		GeoReM values		
	Mean	1 s.d.	Compiled		
CaO	6.54	0.12	6.47		
MgO	7.36	0.28	7.47		
CO ₂	1.34	0.01	1.35		
Na ₂ O	4.68	0.07	4.65		
H ₂ O ⁺	3.92	0.54	3.62		
TiO ₂	1.15	0.02	1.14		
K ₂ O	0.19	0.01	0.20		
BCR-2 (ppm), standard deviation calculated from 3 replicates					
	Measured values		GeoReM values	Recommended	
	Mean	1 s.d.	Range	Mean	1 s.d.
Li	8.83	0.26	9.3	9	2
Sc	31.8	1.0	32.1–38.5, 4 values	33	2
V	386	12	399–477, 6 values	416	14
Cr	19.1	0.6	15.1–66, 4 values	18	2
Co	34.6	1.0	36.8–41, 5 values	37	3
Cu	18.2	0.5	15.6–22, 7 values	21	1
Rb	43.7	1.3	45.5–49.6, 9 values	46.9	0.1
Sr	312	9	312–366, 13 values	340	3
Y	36.1	1.1	28.4–37.2, 7 values	37	2
Zr	184	6	151–250, 11 values	184	1
Nb	12.7	0.4	12.2–14.05, 8 values	12.6	0.4
Cs	1.2	0.04	0.93–1.12, 5 values	1.1	0.1
Ba	653	20	675–692, 8 values	677	2
Hf	4.7	0.1	4.7–5.45, 16 values	4.9	0.1
Ta	0.7	0.02	0.7–0.92, 7 values	0.74	0.02
Pb	11.9	0.4	9.5–13, 7 values	11	1
Th	6.2	0.2	5.23–6.63, 9 values	5.7	0.5
U	1.7	0.1	1.63–1.77, 7 values	1.69	0.19
La	24.7	0.7	23–26.4, 12 values	24.9	0.2
Ce	53.7	1.6	46–55.9, 11 values	52.9	0.2
Pr	7.3	0.2	6.57–15, 9 values	6.7	0.1
Nd	31.4	0.9	26.7–29.9, 13 values	28.7	0.1
Sm	7.3	0.2	6.41–7, 11 values	6.58	0.02
Eu	2.4	0.1	1.688–2.06, 10 values	1.96	0.01
Gd	6.5	0.2	6.14–7.17, 11 values	6.75	0.03
Tb	2.0	0.1	0.97–1.09, 8 values	1.07	0.03
Dy	6.6	0.2	5.99–6.96, 10 values	6.41	0.05
Ho	1.4	0.04	1.21–1.41, 7 values	1.28	0.03
Er	4.4	0.1	3.57–3.96, 10 values	3.66	0.01
Tm	0.6	0.02	0.49–0.83, 6 values	0.54	0.04
Yb	4.0	0.1	3.29–3.48, 11 values	3.38	0.02
Lu	0.6	0.02	0.494–0.54, 15 values	0.503	0.009
JB-2 and ZGI-BM (ppm), internal uncertainty for 1 measurement					
	Measured values		GeoReM values		
	Mean	1 s.d.	Range		
Ni in JB-2	15	0.1	9.0–18.3, 10 values		
Ni in ZGI-BM	58	0.5	57–69, 2 values		

titration—Si, Al, Fe²⁺, Mg, Ca; FAAS—Ti, Mn, Na, K; photometry—Fe³⁺, P; ion selective electrode—F⁻; coulometry—CO₂ and gravimetry—H₂O⁺, H₂O⁻. Mean values and corresponding 1 s.d. uncertainties in wt.% for 20 repeat measurements of the NIST-688 basalt and 14 repeat measurements of the ZGI-BM basalt together with the GeoReM reference values

(Jochum et al., 2005) are given in Table A1. Relative precision of individual analyses given in Table A1 is better than 5%.

Also shown in this table are the results of X-ray fluorescence analysis of Ni in the ZGI-BM and JB-2 basaltic standard reference samples; the relative precision of individual SRM and sample analyses was better than 0.9% (1 s.d.).

Mean values of trace element concentrations (in ppm) calculated from two ICP-MS measurements of the BCR-2 basaltic standard reference material and the corresponding GeoReM values are given in Table A1. The relative precision of individual SRM and sample ICP-MS trace element analyses calculated from 3 repeat measurements (each 5 spectrum sweeps) was better than 3% (1 s.d.).

References

- Armiotti, P., Gasperini, D., 2007. Do we really need mantle components to define mantle composition? *J. Petrol.* 48, 693–709.
- Barker, D.H.N., Austin Jr., J.A., 1998. Rift propagation, detachment faulting, and associated magmatism in Bransfield Strait, Antarctic Peninsula. *J. Geophys. Res.* 103, 24017–24043.
- Ben Othman, D., White, W.M., Patchett, J., 1989. The geochemistry of marine sediments, island arc magma genesis, and crust–mantle recycling. *Earth Planet. Sci. Lett.* 94, 1–21.
- Bibby, J.S., 1966. The stratigraphy of part of north-east Graham Land and the James Ross Island group. *British Antarctic Survey Scientific Reports*, No. 53 (37 pp.).
- Birkenmajer, K., Francalanci, L., Peccerillo, A., 1991. Petrological and geochemical constraints on the genesis of Mesozoic–Cenozoic magmatism of King George Island, South Shetland Islands, Antarctica. *Antar. Sci.* 3, 293–308.
- Bouman, C., Elliott, T., Vroon, P.Z., 2004. Lithium inputs to subduction zones. *Chem. Geol.* 212, 59–79.
- Chan, L.H., Edmond, J.M., Thompson, G., Gillis, K., 1992. Lithium isotopic composition of submarine basalts: implication for the lithium cycle in the oceans. *Earth Planet. Sci. Lett.* 108, 151–160.
- Chan, L.H., Alt, J.C., Teagle, D.A.H., 2002. Lithium and lithium isotope profiles through the upper oceanic crust: a study of seawater–basalt exchange at ODP sites 504B and 896A. *Earth Planet. Sci. Lett.* 201, 187–201.
- Chan, L.H., Frey, F.A., 2003. Lithium isotope geochemistry of the Hawaiian plume: Results from the Hawaii Scientific Drilling Project and Koolau volcano. *Geochim. Geophys. Geosyst.* 4, 8707.
- Chan, L.H., Leeman, W.P., Plank, T., 2006. Lithium isotopic composition of marine sediments. *G-cubed* 7 (6). doi:10.1029/2005GC001202 (paper number Q06005).
- Cohen, A.S., O'Nions, R.K., 1982. Identification of recycled continental material in the mantle from Sr, Nd and Pb isotopic investigations. *Earth Planet. Sci. Lett.* 61, 73–84.
- Cousens, B.L., Allan, J.F., 1992. A Pb, Sr, and Nd isotopic study of basaltic rocks from the Sea of Japan, ODP Leg 127/128. *Proc. Ocean Drilling Program Scientific Results* 127/128, 805–817.
- Crame, J.A., Pirrie, D., Riding, J.B., Thomson, M.R.A., 1991. Campanian–Maastrichtian (Cretaceous) stratigraphy of the James Ross Island area, Antarctica. *J. Geol. Soc. London* 148, 1125–1140.
- Dingle, R.V., Lavelle, M., 1998. Antarctic Peninsula cryosphere: Early Oligocene (c. 30 Ma) initiation and a revised glacial chronology. *J. Geol. Soc. London* 155, 433–437.
- Elliott, T., Thomas, A., Jeffcoate, A., Niu, Y., 2006. Lithium isotope evidence for subduction-enriched mantle in the source of mid-ocean-ridge basalts. *Nature* 443, 565–568.
- Fisk, M.R., 1990. Volcanism in the Bransfield Strait, Antarctica. *J. South Amer. Earth Sci.* 3, 91–101.
- Flesch, G.D., Anderson, A.R., Svec, H.J., 1973. A secondary isotopic standard for ⁶Li/⁷Li determinations. *Int. J. Mass Spectrom. Ion Phys* 12, 265–272.
- Fretzdorff, S., Worthington, T.J., Haase, K.M., Hékinian, R., Franz, L., Keller, R.A., Stoffers, P., 2004. Magmatism in the Bransfield Basin: Rifting of the South Shetland Arc? *J. Geophys. Res.* 109, B12208.
- Gribble, R.F., Stern, R.J., Newman, S., Bloomer, S.H., O'Hearn, T., 1998. Chemical and isotopic composition of lavas from the northern Mariana Trough: implications for magma genesis in back-arc basin. *J. Petrol.* 39, 125–154.
- Guangfu, X., Weizhou, S., Dezi, W., Qingmin, J., 1997. Sr–Nd–Pb isotopes of Tertiary volcanics of King George Island, Antarctica. *Chin. Sci. Bull.* 42, 1913–1918.
- Hanan, B.B., Kingsley, R.H., Schilling, J.G., 1986. Pb isotope evidence in the South Atlantic for migrating ridge-hotspot interactions. *Nature* 322, 137–144.
- Hart, S.R., Blusztajn, J., Craddock, C., 1995. Cenozoic volcanism in Antarctica: Jones Mountains and Peter I Island. *Geochim. Cosmochim. Acta.* 59, 3379–3388.
- Hathway, B., 2000. Continental rift to back-arc basin: Jurassic–Cretaceous stratigraphical and structural evolution of the Larsen Basin, Antarctic Peninsula. *J. Geol. Soc. London* 157, 417–432.
- Hawkins, J.W., Lonsdale, P.F., Macdougall, J.D., Volpe, A.M., 1990. Petrology of the axial ridge of the Mariana Trough backarc spreading center. *Earth Planet. Sci. Lett.* 100, 226–250.
- Hole, M.J., 1988. Post-subduction alkaline volcanism along the Antarctic Peninsula. *J. Geol. Soc. London* 145, 985–988.
- Hole, M.J., 1990. Geochemical evolution of Pliocene–Recent postsubduction alkalic basalts from Seal Nunataks, Antarctic Peninsula. *J. Volcan. Geother. Res.* 40, 149–167.

- Hole, M.J., Smellie, J.L., Mariner, G.F., 1991a. Geochemistry and tectonic setting of alkali-basalts from Alexander Island. In: Thomson, M.R.A., Crame, J.A., Thomson, J.W. (Eds.), *Geological Evolution of Antarctica*. Cambridge University Press, Cambridge, pp. 521–526.
- Hole, M.J., Rogers, G., Saunders, A.D., Storey, M., 1991b. The relationship between alkalic volcanism and slab window formation. *Geology* 19, 657–660.
- Hole, M.J., Kempton, P.D., Millar, I.L., 1993. Trace element and isotope characteristics of small degree melts of the asthenosphere: evidence from the alkalic basalts of the Antarctic Peninsula. *Chem. Geol.* 109, 51–68.
- Hole, M.J., LeMasurier, W.E., 1994. Tectonic controls on the geochemical composition of Cenozoic, mafic alkaline volcanic rocks from West Antarctica. *Contrib. Mineral. Petrol.* 117, 187–202.
- Hole, M.J.H., Saunders, A.D., Rogers, G., Sykes, M.A., 1995. The relationship between alkaline magmatism, lithospheric extension and slab window formation along continental destructive plate margins. In: Smellie, J.L. (Ed.), *Volcanism Associated with Extension at Consuming Plate Margins*, vol. 81. *Geol. Soc. London Spec. Publ.*, London, pp. 265–285.
- Jarrard, R.D., 1986. Relations among subduction parameters. *Reviews of Geophysics* 24, 217–284.
- Jeffcoate, A.B., Elliott, T., Thomas, A., Bouman, C., 2004. Precise, small sample size determinations of lithium isotopic compositions of geological reference materials and modern seawater by MC-ICP-MS. *Geost. Geoanal. Res.* 28, 161–172.
- Jeffcoate, A.B., Elliott, T., Kasemann, S.A., Ionov, D., Cooper, K.M., 2007. Li isotope fractionation in peridotites and mafic melts. *Geochim. Cosmochim. Acta* 71, 202–218.
- Jochum, K.P., Nohl, U., Herwig, K., Lammel, E., Stoll, B., Hofmann, A.W., 2005. GeoREM: a new geochemical database for reference materials and isotopic standards. *Geost. Geoanal. Res.* 29, 333–338.
- Jonkers, H.A., Kelley, S.P., 1998. A reassessment of the age of the Cockburn Island Formation, northern Antarctic Peninsula, and its palaeoclimatic implications. *J. Geol. Soc. London* 155, 737–740.
- Kelemen, P.B., Hanghøj, K., Greene, A.R., 2003. One view of the geochemistry of subduction-related magmatic arcs, with an emphasis on primitive andesite and lower crust. In: Holland, H.D., Turekian, K.K. (Eds.), *Treatise on Geochemistry*, vol. 3. Elsevier, Amsterdam, pp. 593–659.
- Keller, R.A., Fisk, M.R., Smellie, J.L., Strelin, J.A., Lawyer, L.A., White, W.M., 2002. Geochemistry of back arc basin volcanism in Bransfield Strait, Antarctica: subducted contributions and along-axis variations. *J. Geophys. Res.* 107 (B8), 2171. doi:10.1029/2001JB000444.
- Keller, R.A., Fisk, M.R., White, W.M., Birkenmajer, K., 1992. Isotopic and trace element variations on mixing and melting models of marginal basin volcanism, Bransfield Strait, Antarctica. *Earth Planet. Sci. Lett.* 111, 287–303.
- Kent, A.J.R., Elliott, T.R., 2002. Melt inclusions from Marianas arc lavas: implications for the composition and formation of island arc magmas. *Chem. Geol.* 183, 263–286.
- Klein, E.M., 2003. Geochemistry of the igneous oceanic crust. In: Holland, H.D., Turekian, K.K. (Eds.), *Treatise on Geochemistry*, vol. 3. Elsevier, Amsterdam, pp. 433–463.
- Kristjánsson, L., Gudmunsson, M.T., Smellie, J.L., McIntosh, W.C., Esser, R., 2005. Palaeomagnetic, $^{40}\text{Ar}/^{39}\text{Ar}$, and stratigraphical correlation of Miocene–Pliocene basalts in the Brandy Bay area, James Ross Island, Antarctica. *Antar. Sci.* 17, 409–417.
- Larter, R.D., 1991. Debate: Preliminary results of seismic reflection investigations and associated geophysical studies in the area of the Antarctic Peninsula. *Antar. Sci.* 3, 217–220.
- Leat, P.T., Livermore, R.A., Millar, I.L., Pearce, J.A., 2000. Magma supply in back-arc spreading centre segment E2, East Scotia Ridge. *J. Petrol.* 41, 845–866.
- Lee, M.J., Lee, J.I., Choe, W.H., Park, C.H., 2008. Trace element and isotopic evidence for temporal changes of the mantle sources in the South Shetland Islands, Antarctica. *Geochem. J.* 42, 207–219.
- Leeman, W.P., Tonarini, S., Chan, L.H., Borg, L.E., 2004. Boron and lithium isotopic variations in a hot subduction zone – the southern Washington Cascades. *Chem. Geol.* 212, 101–124.
- Machado, A., Chemale Jr., F., Conceição, R.V., Kawaskita, K., Morata, D., Oteiza, O., Van Schmus, W.R., 2005. Modeling of subduction components in the genesis of the Meso-Cenozoic igneous rocks from the South Shetland Arc, Antarctica. *Lithos* 82, 435–453.
- Magna, T., Wiechert, U.H., Halliday, A.N., 2004. Low-blank separation and isotope ratio measurement of small samples of lithium using multiple-collector ICPMS. *Int. J. Mass Spectrom.* 239, 67–76.
- Magna, T., Wiechert, U., Grove, T.L., Halliday, A.N., 2006a. Lithium isotope fractionation in the Southern Cascadia subduction zone. *Earth Planet. Sci. Lett.* 250, 428–443.
- Magna, T., Wiechert, U., Halliday, A.N., 2006b. New constraints on the lithium isotope compositions of the Moon and terrestrial planets. *Earth Planet. Sci. Lett.* 243, 336–353.
- Marschall, H.R., Pogge von Strandmann, P.A.E., Seitz, H.M., Elliott, T., Niu, Y., 2007. The lithium isotopic composition of orogenic eclogites and deep subducted slabs. *Earth Planet. Sci. Lett.* 262, 563–580.
- McCarron, J.J., Smellie, J.L., 1998. Tectonic implications of forearc magmatism and generation of high-magnesian andesites: Alexander Island, Antarctica. *J. Geol. Soc. London* 155, 269–280.
- McCarron, J.J., Larter, R.D., 1998. Late Cretaceous to early Tertiary subduction history of the Antarctic Peninsula. *J. Geol. Soc. London* 155, 255–268.
- Moriguti, T., Nakamura, E., 1998. Across-arc variation of Li isotopes in lavas and implications for crust/mantle recycling at subduction zones. *Earth Planet. Sci. Lett.* 163, 167–174.
- Moriguti, T., Shibata, T., Nakamura, E., 2004. Lithium, boron and lead isotope and trace element systematics of Quaternary basaltic volcanic rocks in northeastern Japan: mineralogical controls on slab-derived fluid composition. *Chem. Geol.* 212, 81–100.
- Nelson, P.H.H., 1966. The James Ross Island Volcanic Group of North-East Graham Land. *British Antarctic Survey Scientific Report*, No. 54. 62 pp.
- Nishio, Y., Nakai, S., Yamamoto, J., Sumino, H., Matsumoto, T., Prikhod'ko, V.S., Arai, S., 2004. Lithium isotopic systematics of the mantle-derived ultramafic xenoliths: implications for EM1 origin. *Earth Planet. Sci. Lett.* 217, 245–261.
- Nishio, Y., Nakai, S., Ishii, T., Sano, Y., 2007. Isotopic systematics of Li, Sr, Nd and volatiles in Indian Ocean MORBs of the Rodrigues Triple Junction: Constraints on the origin of DUPAL anomaly. *Geochim. Cosmochim. Acta.* 71, 745–759.
- Pearce, J.A., Peate, D.W., 1995. Tectonic implications of the composition of volcanic arc magmas. *Ann. Rev. Earth Planet. Sci.* 23, 251–285.
- Peate, D.W., Kokfelt, T.F., Hawkesworth, C.J., van Calsteren, P.W., Hergt, J.M., Pearce, J.A., 2001. U-series isotope data on Lau Basin glasses: the role of subduction-related fluids during melt generation in back-arc basins. *J. Petrol.* 42, 1449–1470.
- Peccerillo, A., Taylor, S.R., 1976. Geochemistry of Eocene calcalkaline volcanic rocks from the Kastamonu area, northern Turkey. *Contrib. Mineral. Petrol.* 58, 63–81.
- Pin, C., Briot, D., Bassin, C., Poitrasson, F., 1994. Concomitant separation of strontium and samarium–neodymium for isotope analyses in silicate samples, based on specific extraction chromatography. *Anal. Chim. Acta.* 298, 209–217.
- Pirrie, D., 1994. Petrography and provenance of the Marambio Group, Vega Island, Antarctica. *Antar. Sci.* 6, 517–527.
- Plank, T., 2005. Constraints from thorium/lanthanum on sediment recycling at subduction zones and the evolution of the continents. *J. Petrol.* 46, 921–944.
- Richard, P., Shimizu, N., Allègre, C.J., 1976. $^{143}\text{Nd}/^{146}\text{Nd}$, a natural tracer: an application to oceanic basalts. *Earth Planet. Sci. Lett.* 31, 269–278.
- Rocholl, A., Stein, M., Molzahn, M., Hart, S.R., Worner, G., 1995. Geochemical evolution of rift magmas by progressive tapping of a stratified mantle source beneath the Ross Sea Rift, Northern Victoria Land, Antarctica. *Earth Planet. Sci. Lett.* 131, 207–224.
- Rosner, M., Ball, L., Peucker-Ehrenbrink, B., Bluzstajn, J., Bach, W., Erzinger, J., 2007. A simplified, accurate and fast method for lithium isotope analysis of rocks and fluids, and $\delta^7\text{Li}$ values of seawater and rock reference materials. *Geost. Geoanal. Res.* 31, 77–88.
- Ryan, J.G., Kyle, P.R., 2004. Lithium abundance and lithium isotope variations in mantle sources: insights from intraplate volcanic rocks from Ross Island and Marie Byrd Land (Antarctica) and other oceanic islands. *Chem. Geol.* 212, 125–142.
- Rudnick, R.L., Ionov, D.A., 2007. Lithium elemental and isotopic disequilibrium in minerals from peridotite xenoliths from far-east Russia: product of recent melt/fluid-rock reaction. *Earth Planet. Sci. Lett.* 256, 278–293.
- Saunders, A.D., Tarney, J., 1979. The geochemistry of basalts from a back-arc spreading centre in the East Scotia Sea. *Geochim. Cosmochim. Acta.* 43, 555–572.
- Saunders, A.D., Tarney, J., 1984. Geochemical characteristics of basaltic volcanism within back-arc basins. In: Kokelaar, B.P., Howells, M.F. (Eds.), *Marginal Basin Geology: Volcanic and Associated Sedimentary and Tectonic Processes in Modern and Ancient Marginal Basins*. *Geol. Soc. London Spec. Publ.*, vol. 16, pp. 59–76.
- Seitz, H.M., Brey, G.P., Zipfel, J., Ott, U., Weyer, S., Durali, S., Weinbruch, S., 2007. Lithium isotope composition of ordinary and carbonaceous chondrites, and differentiated planetary bodies: bulk solar system and solar reservoirs. *Earth Planet. Sci. Lett.* 260, 582–596.
- Smellie, J.L., 1981. A complete arc-trench system recognized in Gondwana sequences of the Antarctic Peninsula region. *Geol. Mag.* 118, 139–159.
- Smellie, J.L., Pankhurst, R.J., Thomson, M.R.A., Davies, R.E.S., 1984. The geology of the South Shetland Islands: VI. Stratigraphy, geochemistry and evolution. *Brit. Antar. Surv. Sci. Rep.* 87 (85 pp.).
- Smellie, J.L., 1987. Geochemistry and tectonic setting of alkaline volcanic rocks in the Antarctic Peninsula: a review. *J. Volcan. Geother. Res.* 32, 269–285.
- Smellie, J.L., 1999. Lithostratigraphy of Miocene–Recent, alkaline volcanic fields in the Antarctic Peninsula and eastern Ellsworth Land. *Antar. Sci.* 11, 362–378.
- Smellie, J.L., 2006. The relative importance of supraglacial versus subglacial meltwater escape in basaltic subglacial tuya eruptions: an important unresolved conundrum. *Earth Sci. Rev.* 74, 241–268.
- Smellie, J.L., McIntosh, W.C., Esser, R., Fretwell, P., 2006a. The Cape Purvis volcano, Dundee Island (northern Antarctic Peninsula): late Pleistocene age, eruptive processes and implications for a glacial palaeoenvironment. *Antar. Sci.* 18, 399–408.
- Smellie, J.L., MacArthur, J.M., McIntosh, W.C., Esser, R., 2006b. Late Neogene interglacial events in the James Ross Island region, northern Antarctic Peninsula, dated by Ar/Ar and Sr-isotope stratigraphy. *Palaeogeogr. Palaeoclimat. Palaeoecol.* 242, 169–187.
- Stern, R.J., Lin, P.N., Morris, J.D., Jackson, M.C., Fryer, P., Bloomer, S.H., Ito, E., 1990. Enriched back-arc basin basalts from the northern Mariana Trough: implications for the magmatic evolution of back-arc basins. *Earth Planet. Sci. Lett.* 100, 210–225.
- Sun, S.S., McDonough, W.F., 1989. Chemical and isotopic systematics of oceanic basalts: implications for mantle composition and processes. In: Saunders, A.D., Norry, M.J. (Eds.), *Magmatism in the Ocean Basins*. *Geol. Soc. London Spec. Publ.*, vol. 42, pp. 313–345. London.
- Sykes, M.A., 1988a. The petrology and tectonic significance of the James Ross Island Volcanic Group, Antarctica. Ph.D. thesis, University of Nottingham, unpublished.
- Sykes, M.A., 1988b. New K–Ar age determinations on the James Ross Island Volcanic Group, north-east Graham Land, Antarctica. *Brit. Antar. Surv. Bull.* 80, 51–56.
- Tarney, J., Weaver, S.D., Saunders, A.D., Pankhurst, R.J., Barker, P.F., 1982. Volcanic evolution of the northern Antarctic Peninsula and the Scotia arc. In: Thorpe, R.S. (Ed.), *Andesites*. John Wiley, Hoboken, N. J., pp. 371–413.
- Teng, F.Z., McDonough, W.F., Rudnick, R.L., Dalpé, C., Tomascak, P.B., Chappell, B.W., Gao, S., 2004. Lithium isotopic composition and concentration of the upper continental crust. *Geochim. Cosmochim. Acta.* 68, 4167–4178.
- Tomascak, P.B., Carlson, R.W., Shirey, S.B., 1999a. Accurate and precise determination of Li isotopic compositions by multi-collector sector ICP-MS. *Chem. Geol.* 158, 145–154.
- Tomascak, P.B., Tera, F., Helz, R.T., Walker, R.J., 1999b. The absence of lithium isotope fractionation during basalt differentiation: new measurements by multicollector sector ICP-MS. *Geochim. Cosmochim. Acta.* 63, 907–910.
- Tomascak, P.B., Widom, E., Benton, L.D., Goldstein, S.L., Ryan, J.G., 2002. The control of lithium budgets in island arcs. *Earth Planet. Sci. Lett.* 196, 227–238.

- Tomascak, P.B., Langmuir, C.H., LeRoux, P., Shirey, S.B., 2008. Lithium isotopes in global mid-ocean ridge basalts. *Geochim. Cosmochim. Acta.* 72 (6), 1626–1637.
- Turner, S., Hawkesworth, C., 1998. Using geochemistry to map mantle flow beneath the Lau Basin. *Geology* 26, 1019–1022.
- Volpe, A.M., Macdougall, J.D., Lugmair, G.W., Hawkins, J.W., Lonsdale, P.F., 1990. Fine-scale isotopic variation in Mariana Trough basalts: evidence for heterogeneity and a recycled component in backarc basin mantle. *Earth Planet. Sci. Lett.* 100, 251–264.
- Williams, M., Smellie, J.L., Johnson, J.S., Blake, D.B., 2006. Late Miocene Asterozoans (Echinodermata) from the James Ross Island Volcanic Group. *Antar. Sci.* 18, 117–122.
- Woodhead, J., Eggins, S., Gamble, J., 1993. High field strength and transition element systematics in island arc and back-arc basin basalts: evidence for multi-phase melt extraction and a depleted mantle wedge. *Earth Planet. Sci. Lett.* 114, 491–504.
- Zack, T., Tomascak, P.B., Rudnick, R.L., Dalpé, C., McDonough, W.F., 2003. Extremely light Li in orogenic eclogites: the role of isotope fractionation during dehydration in subducted oceanic crust. *Earth Planet. Sci. Lett.* 208, 279–290.
- Zindler, A., Hart, S.R., 1986. Chemical geodynamics. *Ann. Rev. Earth Planet. Sci.* 14, 493–571.